Available online at www.sciencedirect.com
SCIENCE DIRECT®
Journal of the European Ceramic Society 25 (2005) 283–286
www.elsevier.com/locate/jeurceramsoc

Phase separation in sol–gel derived ZrO_2–SiO_2 nanostructured materials

A. Gaudon, A. Dauger, A. Lecomte, B. Soulestin, R. Guinebretière*

Science des Procédés Céramiques et de Traitements de Surface—UMR CNRS no. 6638 ENSCI, 47 Avenue Albert Thomas—87065 Limoges, France

Available online 13 September 2004

Abstract

Textures formed by phase separation and crystallization of sol–gel derived ZrO_2–SiO_2 materials with 30 mol% ZrO_2, were examined by X-ray diffraction, small angle X-ray scattering and transmission electron microscopy. An amorphous phase separation consisting in silica-rich and zirconia-rich interconnected domains was shown to be present before crystallization. In the initial stage crystallization of metastable tetragonal zirconia, nucleation was considered to occur in the ZrO_2-rich regions. The size and spatial distribution of crystalline particles, dispersed in the amorphous SiO_2-rich matrix, are controlled by the phase separation texture.

Keywords: Phase separation; X-Ray diffraction; Crystallization

1. Introduction

ZrO_2–SiO_2 mixed oxides are promising materials to be used in a broad spectrum of applications including catalytic processes,[1–4] high permittivity insulating films,[5–8] high fracture toughness glass ceramics[9] and a variety of optical coatings.[10–12] Most of these applications require the fabrication of thin layers. The sol–gel methods are very often used for the preparation of such mixed oxide coatings, because it is a low-cost process, with inexpensive equipments and it could be easily converted to industrial scale. The main advantage of sol–gel processing is the high degree of compositional and homogeneity control inherent with the solution synthesis of multi-component inorganic materials. The potential for microstructure control is great.

The behavior of sol–gel ZrO_2–SiO_2 derived materials has been widely studied.[13–17] Many investigators have reported that low-temperature deposition usually yields amorphous films, but during device fabrication, films have to withstand temperatures above the crystallization temperature of the binary oxides system. This result in a composite microstructure consisting of a crystalline ZrO_2-rich phase embedded in a SiO_2-rich matrix. Such a microstructure is sometimes favorable and sometimes unfavorable to the expected properties of the material. Therefore, in both cases, it would be useful to control the crystallization conditions of the zirconia grains.

To date, the existence of a liquid miscibility gap in the ZrO_2–SiO_2 phase diagram is accepted. Furthermore, the extension of this liquid immiscibility as a metastable miscibility gap in solid state has frequently been suggested. It was recently confirmed by simulation of the thermodynamics of mixing in the ZrO_2–SiO_2 liquid solution.[18]

So, it is necessary to investigate the phase separation and crystallization process precisely, in sol–gel derived ZrO_2–SiO_2 system. The metastable immiscibility should influence the crystallization of zirconia and the phase-separated texture should control the microstructure of the resulting nanocomposite material. Transmission electron microscopy (TEM) and small angle X-ray scattering (SAXS) are suitable techniques because the expected size of the texture ranges from 1 to 50 nm. Moreover, SAXS is well-suited for studying spinodal decomposition mechanism which is expected inside a metastable miscibility gap.[19]

In this work, the texture formed by phase separation in 30 mol% ZrO_2–SiO_2 xerogels and crystallization of the metastable tetragonal zirconia phase were examined by SAXS, TEM and X-ray diffraction (XRD).

* Corresponding author. Tel.: +33 5 55 45 22 07; fax: +33 5 55 79 09 98.
E-mail address: r_guinebretiere@ensci.fr (R. Guinebretière).

0955-2219/$ – see front matter © 2004 Elsevier Ltd. All rights reserved.
doi:10.1016/j.jeurceramsoc.2004.08.010

2. Experimental procedure

2.1. Material synthesis

For this study, ZrO_2–SiO_2 gels with 30 mol% ZrO_2 were prepared in acidic conditions, with alkoxides as starting precursors. All the sols were synthesized in a dry atmosphere to avoid uncontrolled hydrolysis from tetraethyl-orthosilicate (Teos: $Si(OEt)_4$, Aldrich Chemicals), zirconium *n*-propoxide ($Zr(OPr)_4$, Alfa Products) and acetylacetone (acac: $C_5H_8O_2$, Merk) as chelating agent for the zirconium *n*-propoxide.[20]

The reaction rate of silica and zirconia precursors toward water is quite different; silicon alkoxide without any catalyst is "stable" over a long period of time before gelation begins, while zirconium alkoxide reacts immediately. To match their reactivity, the silica precursor solution was pre-hydrolyzed at room temperature under mechanical stirring. Then, the chelated zirconia precursor solution was slowly added while continuously stirring. And finally the final amount of H_2O is slowly mixed. The sol parameters were the concentration in alkoxides, $C = [Zr(OPr)_4] + [Si(OEt)_4] = 0.5\,mol\,L^{-1}$, the hydrolysis ratio W = [water]/[alkoxides] = 10, and the complexing ratio R = [acac]/[$Zr(OPr)_4$] = 0.7.

The sols gelled after few hours at 60 °C. The gels were slowly dried at 60 °C under a 100% humidity atmosphere in order to form massive xerogels, as proposed by Nogami.[21] Resulting samples were then fired at 600 and 1000 °C for various times. XRD and SAXS experiments were carried out on optically polished small slices about 100 μm in thickness (Fig. 1).

2.2. Characterization

SAXS measurements were performed using a point like collimation geometry. The monochromatic X-ray incident beam was provided by a double channel cut germanium monochromator adapted to a 12 kW rotating anode with a Cu target. The scattered intensities were recorded using a linear position sensitive detector (Elphyse). The sample to detector distance, fixed to 0.5 m, allows to cover a q-range from 0.1 to 4 nm^{-1} where q is the scattering vector, $q = 4\pi\lambda^{-1}\sin(\theta)$, λ is the Cu Kα1 wavelength and 2θ is the scattering angle.[22]

XRD experiments were carried out in a Debye–Scherrer geometry based diffractometer with a sealed tube operating at 37.5 kV/28 mA, a quartz monochromator (Cu Kα1 radiation) and equipped with a curved position sensitive detector (Inel CPS 120).[23] The mean crystallite size was determined using the integral breadth method.[24] Due to the X-ray diffraction line overlapping, the pattern simulations were done by Rietveld refinement[25] using the Fullprof package.[26] Instrumental broadening was estimated using the Nist profile standard 660 LaB_6.

The morphology and texture were also investigated using a Jeol 2010 transmission electron microscope operating at 200 kV.

3. Results and discussion

As previously observed,[13–15] the dried gels obtained after 1 h at 600 °C exhibit a "non diffracting" structure (Fig. 2) and we can consider that the xerogel is amorphous, even if its chemical composition is perhaps not yet that of pure ZrO_2–SiO_2 mixed oxides.

Further investigation of this xerogel monolith shows that the material is not homogeneous at a nanometric scale. As a matter of fact, the SAXS intensity distribution (Fig. 3a) clearly shows a peak at q_m = 0.3–0.4 nm^{-1} corresponding to a correlation length of about 18 nm in direct space. A SAXS curve being the fourier transform of the electron density distribution within the observed sample, the only requirement for SAXS intensity appearance is the presence of inhomogeneities in electron density with colloidal size, such as particles, pores or compositional fluctuations. The main difficulty is to extract information about the nature, the shape and the spatial distribution of these inhomogeneities. In the present case, TEM observations (Fig. 3b) prove that com-

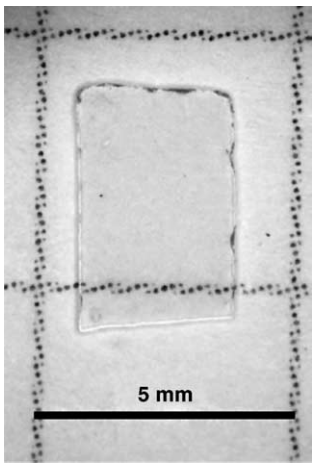

Fig. 1. Optical photograph of a monolithic xerogel sample dried at 600 °C for 1 h.

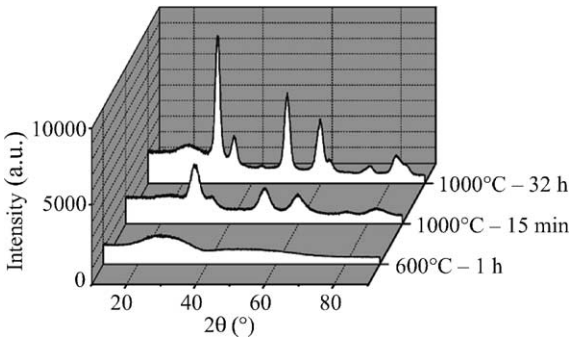

Fig. 2. XRD patterns for samples heated at 600 and 1000 °C. At 600 °C xerogels are amorphous and only tetragonal zirconia is formed even for long times at 1000 °C.

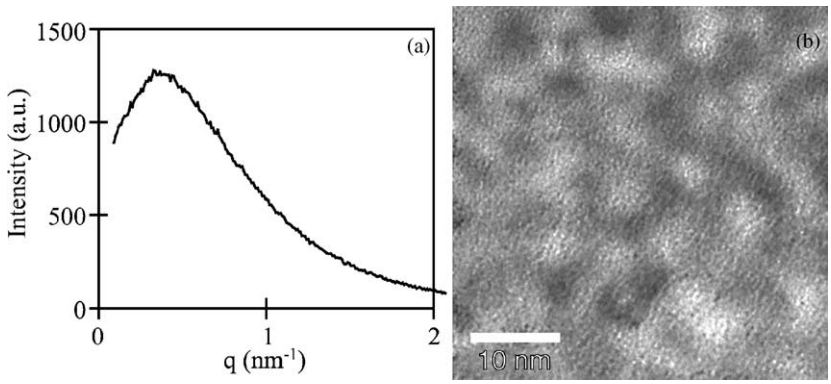

Fig. 3. SAXS intensity distribution (a) and corresponding TEM micrograph (b) for the xerogel treated for 1 h at 600 °C. The sample exhibits a correlation length (18 nm) related to the bicontinuous phase-separated morphology with interconnected zirconia and silica-rich regions.

positional fluctuations are the cause of scattered intensity. The material is amorphous and its microstructure is that of a bi-continuous phase-separated system consisting probably in interconnected ZrO_2-rich and SiO_2-rich domains as expected from a spinodal decomposition mechanism.

Annealing the xerogel at 1000 °C leads immediately to crystallization (Fig. 2). Small crystals of the metastable tetragonal ZrO_2 type phase appear with a mean grain size of about 2.5 nm after an annealing time of 15 min, as determined from XRD measurements. These results are confirmed by TEM observations (Fig. 4a). Moreover, TEM micrographs show that the spatial distribution of the ZrO_2-rich crystals is not random. The previously formed interconnected texture constitutes the matrix from which the crystallization appears. The nucleation of metastable tetragonal ZrO_2-rich particles occurs in the ZrO_2-rich phase. The SAXS curve of the monolithic sample fired for 15 min at 1000 °C exhibits a rather unusual intensity distribution with the coexistence of two peaks (Fig. 4b). The first one, located at q_{m1} = 0.3–0.4 nm^{-1}, is the same as the previous one that was attributed to amorphous phase separation. Its position corresponds to the typical size of the largest amplification of the compositional fluctuation.[19] This fluctuation does still persist since the ZrO_2-rich crystals are decorating the ZrO_2-rich domains. The second scattered intensity peak, located at q_{m2} = 1–1.2 nm^{-1} is attributed to short-range correlations between the crystalline ZrO_2-rich crystals. The corresponding mean interparticle distance, about 5.8 nm, is in good agreement with the ZrO_2 volume fraction and the crystal size as determined by XRD experiments. This means that these crystalline crystals are very homogeneously distributed in the ZrO_2-rich phase.

Through further annealing at 1000 °C, the growth of the crystalline particles is observed (Fig. 2). Their mean grain sizes were determined from XRD pattern analysis. They grow from 2.5 nm in diameter after 15 min up to about 5 nm after 32 h at 1000 °C. Corresponding SAXS curves are shown in Fig. 5a. The first scattered intensity peak, at q_{m1}, rapidly disappears because of the coarsening of the initial microstructure. The second peak intensity strongly increases since its position goes slowly towards smaller angles, accompanying the crystalline particles growth. All the SAXS curves collapse into a single master curve (Fig. 5b) when plotted as $I(q/q_{m2}(t))(q_{m2}(t))^3$ versus $q/q_{m2}(t)$, showing that

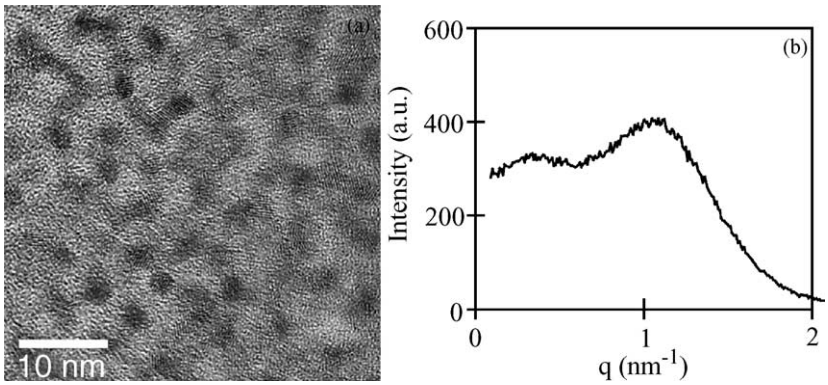

Fig. 4. TEM micrograph (a) and corresponding SAXS curve (b) of a sample fired for 15 min at 1000 °C. The SAXS curve is quite unusual and reveals the existence of two correlation lengths, respectively, 14.3 and 5.8 nm. The first one is related to the bicontinuous phase-separated morphology and the second one is associated to the mean distance between crystalline zirconia particles.

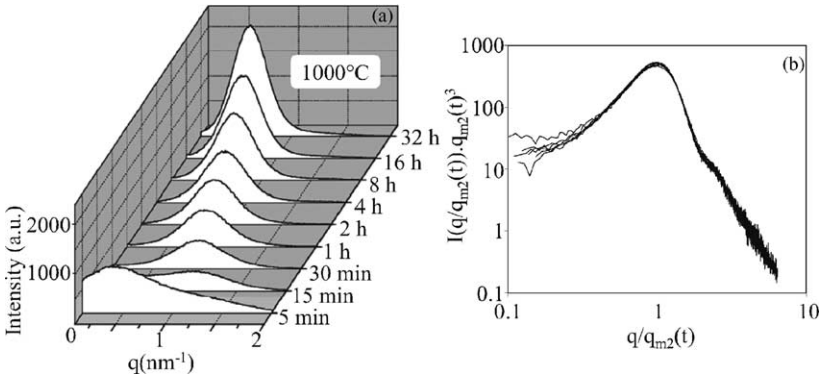

Fig. 5. Evolution of SAXS data during isothermal heat treatments at 1000 °C for 1–32 h at 1000 °C (a) and the corresponding dynamical scaling behavior of the structure factors (b).

the experimental structure factors are time independent and grow with dynamical self-similarity. This scaling behavior is known[27–28] to be followed in the late stages of phase separation after quenching into a miscibility gap. It applies to two-densities systems with constant compositions and volume fractions.

4. Conclusion

The phase separation and crystallization textures formed in sol–gel derived 30 mol% ZrO_2–SiO_2 mixed oxides were examined. Monolithic xerogel samples were studied by XRD experiments, SAXS intensities measurements and TEM observations.

Interconnected textures probably formed by spinodal decomposition appear in the xerogel fired at low temperature, i.e. for 1 h at 600 °C. The crystallization of zirconia-rich nanometric particles, in the metastable tetragonal form, is shown to occur from the zirconia-rich phase previously formed by phase separation. At 1000 °C for 15 min, for example, the microstructure consists of a fine dispersion of very small zirconia-rich crystals, 2.5 nm in diameter, embedded in an amorphous SiO_2-rich matrix. With longer annealing times, the coarsening of the texture and the increase of the inter-ZrO_2-rich crystals distances were observed, XRD and TEM observations being in good agreement with SAXS analysis.

Such a mechanism where the size and spatial distribution of the crystalline particles are controlled by the phase separation texture provides a promising potential to manage the microstructure of functional layers.

Acknowledgements

The authors would like to express their gratitude towards the European Community (the European Social Funds) and the Limousin Region for their financial support of the present work.

References

1. Itoh, M., Hattori, H. and Tanabe, K. J., *J. Catal.*, 1974, **35**, 225.
2. Miller, J. B. and Ko, E. I., *J. Catal.*, 1996, **159**, 58.
3. Lopez, T., Tzompantzi, F., Navarrete, J., Gomez, R., Boldu, J. L. and Munoz, E., *J. Catal.*, 1999, **181**, 285.
4. Zhuang, Q. and Miller, J. M., *Can. J. Chem.*, 2001, **79**, 1220.
5. Stemmer, S., Chen, Z., Levi, C. G., Lysaght, P. S., Foran, B., Gisby, J. A. *et al.*, *Jpn J. Appl. Phys.*, 2003, **42**, 3593.
6. Gusev, E. P., Cartier, E., Buchanan, D. A., Gribelyuk, M., Copel, M., Okorn-Schimdt, H. *et al.*, *Microelectron. Eng.*, 2001, **59**, 341.
7. Lucovsky, G., Rayner, G. B. and Johnson, R. S., *Microelectron. Rel.*, 2001, **41**, 937.
8. Lucovsky, G. and Rayner, G. B., *Appl. Phys. Lett.*, 2000, **77**, 2912.
9. Nogami, M. and Tomozawa, M., *J. Am. Ceram. Soc.*, 1986, **69**, 99.
10. Li, Q., Ai, D., Dai, X. and Wang, J., *Powder Technol.*, 2003, **137**, 34.
11. He, H., Wang, Y., Wang, Y., Zhou, Y., Chen, Z. and Yuan, S., *Solid State Commun.*, 2003, **126**, 639.
12. Song, C. F., Lü, M. K., Yang, P., Gu, F., Xu, D. and Yuan, D. R., *Mat. Sci. Eng. B*, 2002, **94**, 181.
13. Nogami, M., *J. Mater. Sci.*, 1986, **21**, 3513.
14. Aguilar, D. H., Torres-Gonzalez, L. C. and Torres-Martinez, L. M., *J. Solid State Chem.*, 2000, **158**, 349.
15. del Monte, F., Larsen, W. and Mackenzi, J. D., *J. Am. Ceram. Soc.*, 2000, **83**, 628.
16. Stachs, O., Petkov, V. and Gerber, T., *J. Appl. Crystallogr.*, 1997, **30**, 670.
17. Margaça, F. M. A., Miranda Salvado, I. M. and Teixeira, J., *J. Non Cryst. Solids*, 1997, **209**, 143.
18. Kim, H. and McIntyre, P. C., *J. Appl. Phys.*, 2002, **92**, 5094.
19. Takei, T., Kameshima, Y., Yasumori, A., Okada, K., Kumada, N. and Kinomura, N., *J. Non-Cryst. Solids*, 2001, **282**, 265.
20. Lecomte, A., Dauger, A. and Lenormand, P., *J. Appl. Crystallogr.*, 2000, **33**, 496.
21. Nogami, M., *J. Non-Cryst. Solids*, 1985, **69**, 415.
22. Lenormand, P., *Etude de l'évolution microstructurale de précurseurs d'oxyde de zirconium à l'état de gel, xérogel, couche mince et aérogel par diffusion de rayons X*, Thesis, University of Limoges, France, 2001.
23. Masson, O., Guinebretière, R. and Dauger, A., *J. Appl. Crystallogr.*, 1996, **29**, 540.
24. Langford, J. I., *J. Appl. Crystallogr.*, 1978, **11**, 10.
25. Thompson, P., Cox, D. E. and Hasting, J. B., *J. Appl. Crystallogr.*, 1987, **20**, 79.
26. Rodriguez-Carjaval, J., *Fullprof Program.*, 1992.
27. Furukawa, H., *J. Appl. Crystallogr.*, 1988, **21**, 805.
28. Brito, G. E. S., Santilli, C. V., Pulcinelli, S. H. and Craievich, A. F., *J. Non-Cryst. Solids*, 1997, **217**, 41.